JOURNAL OF THEORETICAL
AND APPLIED MECHANICS
43, 2, pp. 385-403, Warsaw 2005

DYNAMIC STABILITY OF THREE-LAYERED ANNULAR PLATE UNDER LATERAL TIME-DEPENDENT LOAD

DOROTA PAWLUS

Department of Mechanical Engineering Fundamentals, University of Bielsko-Biala
e-mail: doro@aristo.pb.bielsko.pl

This paper presents solutions to the problem of behaviour of three-layered annular plates loaded by compressive stress quickly increasing in time acting on the inner plate edge. The finite difference method and finite element method have been used for solving the problem. An axially-symmetrical form of loss of dynamic stability of the plate with clamped inner and outer edges and with a symmetrical transverse structure of layers composed of thin facings and a thicker foam core has been analysed. Using the finite difference method, the basic system of differential equations enabling numerical calculation of plate deflections was formulated. In the finite element method the computational model of an annular sector of the plate fulfilling conditions of the sandwich plate with a soft core has been built. The results of dynamic numerical calculations have been presented in the form of time histories of plate maximum deflection and velocity of deflection. Calculation results of examplary plates differing in thickness and stiffness of the foam core enable qualitative observations of the critical and supercritical plate behaviours with the quantitative evaluation of values of critical parameters: time, deflection and load determined using the criterion presented by Volmir (1972).

Key words: sandwich, annular plate; dynamic stability; increasing load; finite difference method; FEM

1. Introduction

Stress-strain analyses of statically or dynamically loaded annular plates have been undertaken in numerous works. Among them, works concerning plates under plane loads and considering static and dynamic stability problems of homogeneous, elastic or viscoelastic plates could be indicated, see for example

works by Trombski (1972), Wojciech (1978, 1979), Trombski and Wojciech (1981), Dumir and Shingal (1985), Tylikowski (1989), Pawlus (2000).

The wide range of various applications of light, strong and stiff sandwich structures more than once replacing the homogeneous element structure forces one to formulate and solve the deformation problem of sandwich, annular plates, particularly plates under lateral loads. This subject could be a certain complement in the range of rather rarely considered solutions to annular plates with laminar structures. Here, the work concerning moderately thick laminated annular plates subjected to transverse loads presented by Dumir *et al.* (2001) could be specified.

In this paper, solutions to a three-layered annular plate loaded on its surface will be presented. The finite difference method and finite element method are used for solution to the formulated plate problem. Examplary results of calculations enable observation of the critical and supercritical behaviour of plates differing in thickness and stiffness of the foam plate core.

2. Problem formulation

A sandwich annular plate under loading acting on its surface is the subject of consideration. The cross-section structure of the analysed plate is symmetric, composed of three layers: two thin steel facings and one foam, soft, thicker core. The outer loading acts on the edges of plate facings. It is uniformly distributed on plate perimeter.

The loading is linear, quickly increasing, expressed by formula

$$p = st \tag{2.1}$$

where

- p – compressive stress
- s – rate of plate loading growth
- t – time.

The scheme of such a plate model is presented in Fig. 1.

The plate subjected to this kind of loading loses its dynamic stability. As the criterion of loss of plate stability, the criterion presented by Volmir (1972) was adopted. According to this criterion, the loss of plate stability occurs at the moment when the speed of the point of maximum deflection reaches the first maximum value. This accepted criterion of loss of plate stability, concerning the evaluation of values of dynamic critical loads in the region of significant

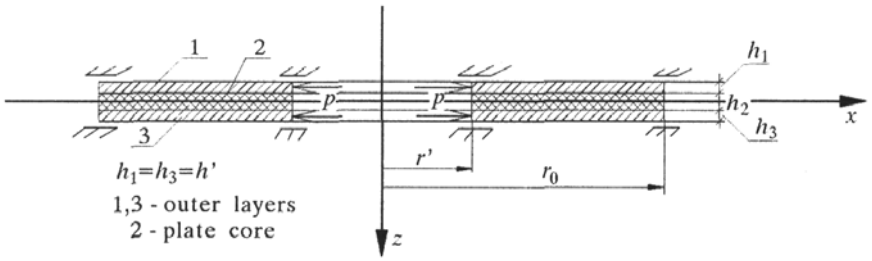

Fig. 1. Scheme of the plate

growth in plate deflections corresponds to the Budiansky-Roth criterion used in analysis of static and dynamic buckling of laminated shells, presented by Tanov and Tabiei (1998) and by Tanov (2000).

The analysed computational example of the plate is for the case of an axially-symmetrical rotational form of the loss stability under compressive stress acting on the inner perimeter of the plate with clamped edges. Calculation results of critical static loads of sandwich plates (Pawlus, 2003b) and critical static and dynamic loads of homogeneous plates (Wojciech, 1978) indicate that the values of critical loads in that case of the axially-symmetrical plate model are minimal.

3. Problem solution

Two solutions of the dynamic stability problem formulated for an axially symmetrical plate will be presented in this paper:

- a solution leading to an expression of the basic system of differential equations describing plate deflections with the use of the approximation finite difference method
- a solution to the calculating model built of finite elements and determination of time histories of plate deflections using the finite element method.

3.1. System of differential equations of three-layered plate

The solution for the analysed model of the three-layered plate is based on the assumption of classical theory of sandwich plate using the broken line hypothesis (Volmir, 1967). The deformation of plate outer layers is described by nonlinear Kármán's plate equations. The thicknesses and material parameters

such as Young's modulus, Poisson's ratio and mass density of plate facings are the same. They are denoted as follows: $h_1 = h_3 = h'$, $E_1 = E_3 = E$, $\nu_1 = \nu_3 = \nu$, $\mu_1 = \mu_3 = \mu$, respectively. Equal values of preliminary and additional deflections of each plate layer are assumed. The material of each layer is represented by linear physical relations of Hooke's law.

The presented solution required:

- formulation of dynamic equilibrium equations for each plate layer
- description of core deformation taking into account preliminary deflection of the plate
- description of physical relations of plate layers
- determination of relations between sectional forces and moments with stresses for plate facings
- determination of resultant transverse Q_r ($Q_r = Q_{r_1} + Q_{r_2} + Q_{r_3}$), radial N_r ($N_r = N_{r_1} + N_{r_3}$), and circumferential N_θ ($N_\theta = N_{\theta_1} + N_{\theta_3}$) forces, which are expressed by the following formulas, respectively

$$Q_r = -2Dw_{d,rrr} - \frac{2D}{r}w_{d,rr} + \frac{2D}{r^2}w_{d,r} + G_2(\delta + H'w_{d,r})\frac{H'}{h_2} \tag{3.1}$$

$$N_r = 2h'\frac{1}{r}\Phi_{,r} \qquad N_\theta = 2h'\Phi_{,rr}$$

where

D	–	flexural rigidity of the outer layer of the plate, $D = Eh'^3/[12(1-\nu^2)]$
E, ν	–	Young's modulus and Poisson's ratio of the facing material, respectively
r	–	plate radius
h', h_2	–	facing and core thicknesses, respectively, ($H' = h' + h_2$, $h = 2h' + h_2$)
w_d	–	additional deflection
G_2	–	Kirchhoff's modulus of the core material
δ	–	difference of radial displacements of middle surfaces of the plate outer layers, which is the resultant of cross-sectional plate structure deformation, presented in Fig. 2, ($\delta = u_3 - u_1$)
$Q_{r_{1(3)}}, Q_{r_2}$	–	transverse forces per unit length of the plate outer layers and core layer, respectively
$N_{r_{1(3)}}, N_{\theta_{1(3)}}$	–	normal radial and circumferential forces per unit length of the outer plate layers, respectively
Φ	–	stresses function

- determination of initial boundary and loading boundary conditions, which are respectively presented by the following expressions

$$\begin{aligned} &w_d|_{t=0} = 0 && (w_d)_{,t}\,|_{t=0} = 0 \\ &w|_{r=r_0(r_i)} = 0 && w_{,r}\,|_{r=r_0(r_i)} = 0 \\ &\delta|_{r=r_0(r_i)} = 0 && \delta_{,r}\,|_{r=r_0(r_i)} = 0 \\ &\sigma_r|_{r=r_i} = -p(t)d_1 && \sigma_r|_{r=r_0} = -p(t)d_2 \end{aligned} \tag{3.2}$$

where

σ_r – radial stress

d_1, d_2 – quantities, which determine the loading of the inner or/and outer plate perimeter – their values are equal: 0 or 1

- assumption of the form of predeflection w_0 according to the formula presented by Wojciech (1978)

$$\zeta_0(\rho) = \xi(\rho^4 + A_1\rho^2 + A_2\rho^2 \ln\rho + A_3 \ln\rho + A_4) \tag{3.3}$$

where

ξ – calibrating number

ζ_0, ρ – dimensionless quantities of predeflection and plate radius, respectively, $\zeta_0 = w_0/h$, $\rho = r/r_0$

A_i – quantities fulfilling the conditions of clamped edges, $i = 1, 2, 3, 4$.

The basic system of differential equations of the plate is as follows

$$k_1 w_{d,rrrr} + \frac{2k_1}{r} w_{d,rrr} - \frac{k_1}{r^2} w_{d,rr} + \frac{k_1}{r^3} w_{d,r} - G_2 \frac{H'^2}{h_2} w_{d,rr} - G_2 \frac{1}{r} \frac{H'^2}{h_2} w_{d,r} + \tag{3.4}$$
$$-G_2 \frac{1}{r} \frac{H'}{h_2} \delta - G_2 \frac{H'}{h_2} \delta_{,r} = \frac{2h'}{r} (w_{,r}\, \Phi_{,rr} + \Phi_{,r}\, w_{,rr}) - w_{d,tt} M$$

$$r\Phi_{,rrr} + \Phi_{,rr} - \frac{1}{r}\Phi_{,r} + \frac{1}{2} E \left(\frac{\partial w}{\partial r}\right)^2 = 0 \tag{3.5}$$

$$\frac{Eh'}{1-\nu^2} r\delta_{,rr} + \frac{Eh'}{1-\nu^2} \delta_{,r} - \frac{Eh'}{1-\nu^2} \frac{1}{r} \delta - \frac{2r}{h_2} G_2 \delta - \frac{2r}{h_2} G_2 H' w_{d,r} + \tag{3.6}$$
$$+ w_{,r} \frac{h'}{2} \frac{G_2}{h_2} E_1 + w_{,rr} \frac{h'}{2} \frac{G_2}{h_2} E_2 + w_{,r} \frac{h'}{2} \frac{G_2}{h_2} E_3 + w_{,rr} \frac{h'}{2} \frac{G_2}{h_2} E_4 = 0$$

where

$$k_1 = 2D \qquad M = 2h'\mu + h_2\mu_2$$

and

- μ, μ_2 – mass density of the outer layers material and core material, respectively
- w – total deflection, $w = w_0 + w_d$
- E_1, E_2 – expressions of the parameter δ and geometric parameters and plate initial and additional deflections
- E_3, E_4 – expressions of geometric parameters and plate initial and additional deflections.

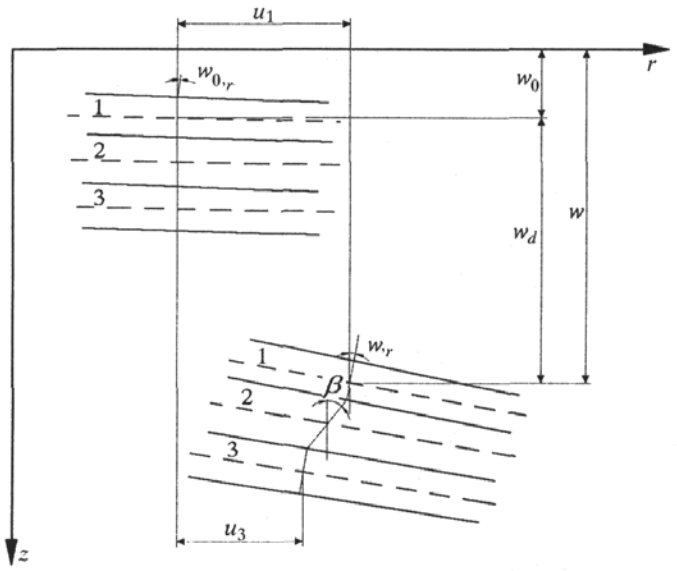

Fig. 2. Cross-sectional geometry of the sandwich plate

Equation (3.4) is a result of the sum of terms of equilibrium equations of projections in the z-axis direction of forces loading the plate layers. Equation (3.5) is an equation of inseparability of deformations. Equation (3.6) is an additional equation which enables calculation of quantity δ existing in equation (3.4). In formulation of equation (3.6), the difference of terms of equilibrium equations of projections in the x-directions of forces loading the facings was used.

A detailed description of the process of solving the analysed plate problem was presented by Pawlus (2003a).

Equations (3.4)-(3.6) were transformed after introducing the following dimensionless quantities and parameters:

— dimensionless plate radius

$$\rho = \frac{r}{r_0}$$

— dimensionless quantities of absolute, additional and preliminary deflections, respectively

$$\zeta = \frac{w}{h} \qquad \zeta_1 = \frac{w_d}{h} \qquad \zeta_0 = \frac{w_0}{h} \tag{3.7}$$

— dimensionless time

$$t^* = tK_7 \tag{3.8}$$

where $K_7 = s/p_{cr}$, and p_{cr} is the critical static stress calculated solving the eigenproblem after neglecting inertial components and initial deflection in equation (3.4), neglecting nonlinear terms and assuming that the stresses function Φ is a solution to the disk state in equation (3.5), see Pawlus (2002a, 2003a).

Replacing the derivatives with respect to ρ by central finite differences in the discrete points, a system of equations has been obtained

$$\mathbf{P}\boldsymbol{U} + \boldsymbol{Q} = K\ddot{\boldsymbol{U}} \qquad \mathbf{F_F}\boldsymbol{Y} = \boldsymbol{U_W} \qquad \mathbf{Z}\boldsymbol{D} = \boldsymbol{V_W} \tag{3.9}$$

where

- K – parameter (b-length of the interval in the finite difference method), $K = b^4 r_0 h_2 h M K_7^2/(G_2 h')$
- $\boldsymbol{U}, \boldsymbol{Y}$ – vectors of additional deflections and components of the stress function, respectively
- $\mathbf{P}$ – matrix with elements composed of geometric and material plate parameters and the quantity b
- $\boldsymbol{Q}$ – vector of expressions composed of the initial and additional deflections, geometric and material parameters, components of stress function, quantity b and coefficient δ
- $\mathbf{F_F}$ – matrix with elements described by the ratio $a_i = b/\rho_i$
- $\boldsymbol{U_W}$ – vector of expressions of the initial and additional deflections, ratio a_i and quantity b
- $\mathbf{Z}$ – matrix of components of plate geometry and plate material parameters, expressions of the initial and additional deflections and quantity b
- $\boldsymbol{D}$ – vector of the coefficient δ
- $\boldsymbol{V_W}$ – vector of components of plate geometry and plate material parameters, expressions of the initial and additional deflections and quantity b.

The system of Eqs (3.9) was solved using Runge-Kutta's integration method for the initial state of the plate in solution to the differential equation

with respect to time $(3.9)_1$, calculating earlier the stress function elements of the vector $\boldsymbol{Y}$ from equation $(3.9)_2$ and the coefficient δ elements of the vector $\boldsymbol{D}$ from equation $(3.9)_3$.

3.2. Calculational model in finite element method

Finite element method calculations were carried out for an annular sector (1/8 part) of the plate formulating proper symmetry conditions.

The selection of grid elements of the plate layers: facings and core was differentiated to assure suitable participation of the plate layers in carrying the basic stresses: normal by the facings and shearing by the core. The remarks presented by Kluesener and Drake (1982) were used. The facings are built of 9-nodes 3D shell elements but the core mesh is built of 27-nodes 3D solid elements, which are arranged in single or double core layers [1]. Schemes of the plate annular sector are presented in Fig. 3.

The grids of outer layers elements are tied with the grid of core elements using the surface contact interaction. The boundary conditions with limitation on the possibility of radial relative displacements in the plate clamped edges are imposed on the outer and inner plate edges. The deformation of individual layers is not limited by a condition of equal deflections of each layer. The form and values of preliminary deflections of the plate layers correspond to the values of plates solved using the method presented above.

The calculations were carried out at the Academic Computer Center CYFRONET-CRACOW (KBN/C3840/CD/034/1996) using the ABAQUS system version 6.3.

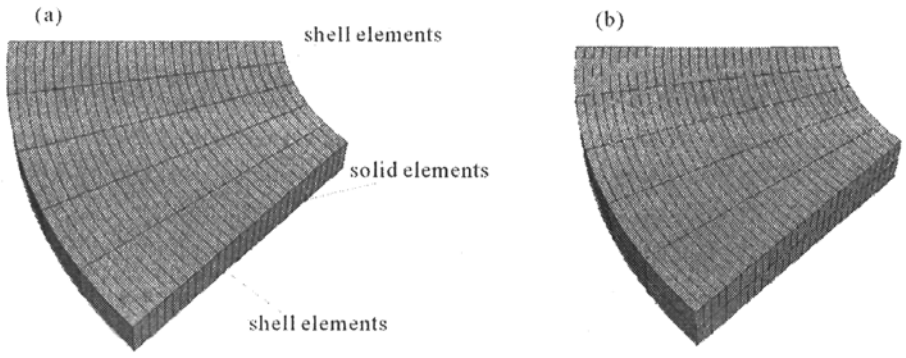

Fig. 3. A model of MES annular sector of plate with core mesh built of single layer (a) and double layer (b) solid elements

4. Examples of numerical calculations

Exemplary numerical calculations were carried out for a plate with the following geometrical dimensions: inner radius $r_i = 0.2\,\mathrm{m}$, outer radius $r_0 = 0.5\,\mathrm{m}$, facing thickness $h' = 0.001\,\mathrm{m}$, core thickness $h_2 = 0.005\,\mathrm{m}$, $0.02\,\mathrm{m}$ or $0.06\,\mathrm{m}$. A steel with parameters: Young's modulus $E = 2.1 \cdot 10^5\,\mathrm{MPa}$, Poisson's ratio $\nu = 0.3$, mass density $\mu = 7.85 \cdot 10^3\,\mathrm{kg/m^3}$ is the facing material. Polyurethane foam is the core material. The accepted material parameters, Kirchhoff's modulus and mass density, for two kinds of foams presented in works by Romanów (1995) and Majewski and Maćkowski (1975) are equal, respectively: $G_2 = 5\,\mathrm{MPa}$ $\mu_2 = 64\,\mathrm{kg/m^3}$, $G_2 = 15.82\,\mathrm{MPa}$ $\mu_2 = 93.6\,\mathrm{kg/m^3}$; according to the standard specification PN-84/B- 03230 the value of Poisson's ratio is equal $\nu = 0.3$; calculated Young's moduli treating the foam material as isotropic are, respectively: $E_2 = 13\,\mathrm{MPa}$, $E_2 = 41.13\,\mathrm{MPa}$.

Rapidly increasing loading acting on the edge is expressed by equation (2.1). The rate of plate loading growth s is equal in each numerical case of the analysed plate. The value of the rate s is the result of the following equation: $s = K_7 p_{cr}$ (3.8). The value of the parameter K_7 is accepted as $K_7 = 20$. Solving the eigenproblem, the value of the critical stress is $p_{cr} = 217.3\,\mathrm{MPa}$ when calculated for the plate with the facing thickness $h' = 0.001\,\mathrm{m}$, core thickness $h_2 = 0.01\,\mathrm{m}$ and core Kirchhoff's modulus $G_2 = 15.82\,\mathrm{MPa}$.

4.1. Results of calculations using finite difference method

Time histories of maximum plate deflections are results of exemplary plate calculations. The marked point in the diagram determines the critical time and critical deflection at the moment of loss of plate stability according to the accepted criterion. The results in the form of curves $\zeta_{1max} = f(t^*)$ are presented in Fig.4.

The calculations were carried out for the number N of discrete points in the finite difference method equal to 14. This value fulfils the accuracy up to 5% of technical error for the critical time t^*_{cr} of the loss of plate dynamic stability. Table 1 shows exemplary values of the critical time t^*_{cr} for different numbers of discrete points: $N = 11, 14, 17, 21, 26$. The geometrical, material and loading parameters of the analysed plate are described above in Section 4. The considered plates differ in geometry and material of their cores. They are characterised by the quantities h_2 and G_2 shown in Fig.4 and given in Table 1 and Table 2.

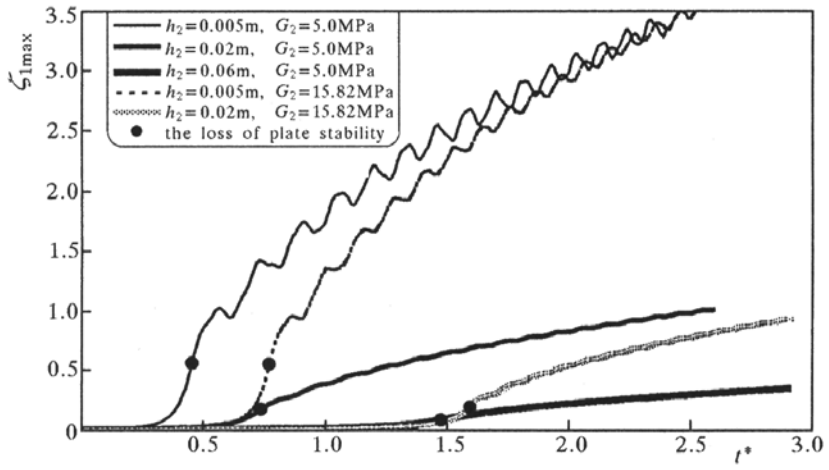

Fig. 4. Time histories of plates with different values of the core thickness h_2 and Kirchhoff's modulus G_2

Table 1. Values of the critical time t^*_{cr} for different numbers N

N	t^*_{cr}	
	Parameters of the plate core h_2 [m]/G_2 [MPa]	
	0.02/15.82	0.06/5.0
11	1.525	1.393
14	1.595	1.469
17	1.615	1.481
21	1.621	1.479
26	1.627	1.473

Table 2. Values of the critical time t_{cr}, deflection w_{dcr} and dynamic loading p_{crdyn} for analysed plate examples

Parameters of the plate core h_2 [m]/G_2 [MPa]	t_{cr} [s]	w_{dcr} [m]	p_{crdyn} [MPa]
0.005/5.0	0.023	$3.92 \cdot 10^{-3}$	99.97
0.02/5.0	0.037	$3.77 \cdot 10^{-3}$	160.82
0.06/5.0	0.074	$5.21 \cdot 10^{-3}$	321.65
0.005/15.82	0.038	$3.87 \cdot 10^{-3}$	165.17
0.02/15.82	0.08	$4.25 \cdot 10^{-3}$	347.73

Values of the critical time t_{cr} and critical additional deflection w_{dcr} determined by making use of equations (3.7) and (3.8) and the critical dynamic loading expressed by the following formula: $p_{crdyn} = st_{cr}$ are presented in Table 2.

4.2. Results of calculations using finite element method

The calculations results are presented in Fig. 5 - Fig. 9 in the form of following curves:

- time history of the plate maximum deflection,
- time history of plate velocity of deflection with a magnified area of time histories of the plate deflection and velocity of deflection in the critical region of plate operation for $h_2 = 0.005\,\mathrm{m}$ and $G_2 = 5\,\mathrm{MPa}$.

These detailed diagrams enable one to readout the critical values: time t_{cr} and deflection w_{dcr}.

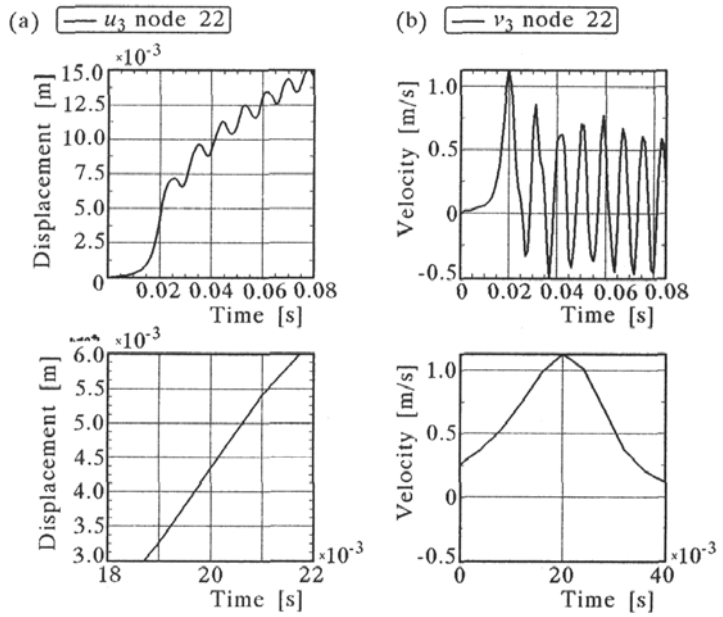

Fig. 5. Time history of deflection (a) and deflection velocity (b) for $h_2 = 0.005\,\mathrm{m}$ and $G_2 = 5.0\,\mathrm{MPa}$

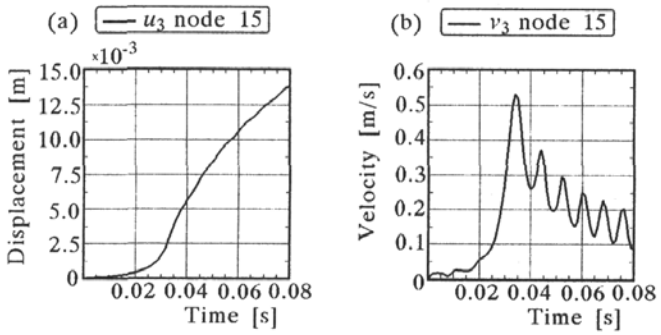

Fig. 6. Time history of deflection (a) and deflection velocity (b) for $h_2 = 0.02\,\mathrm{m}$ and $G_2 = 5.0\,\mathrm{MPa}$

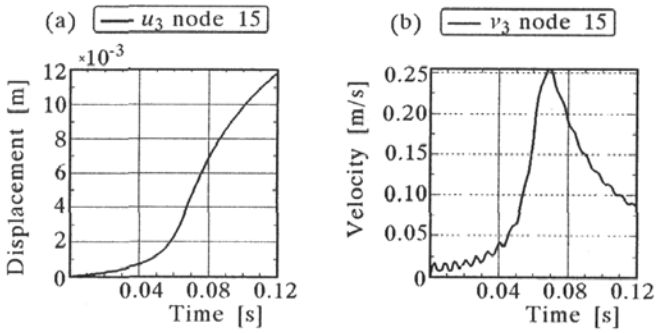

Fig. 7. Time history of deflection (a) and deflection velocity (b) for $h_2 = 0.06\,\mathrm{m}$ and $G_2 = 5.0\,\mathrm{MPa}$

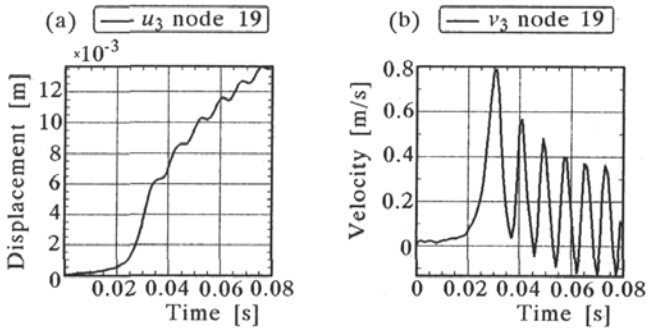

Fig. 8. Time history of deflection (a) and deflection velocity (b) for $h_2 = 0.005\,\mathrm{m}$ and $G_2 = 15.82\,\mathrm{MPa}$

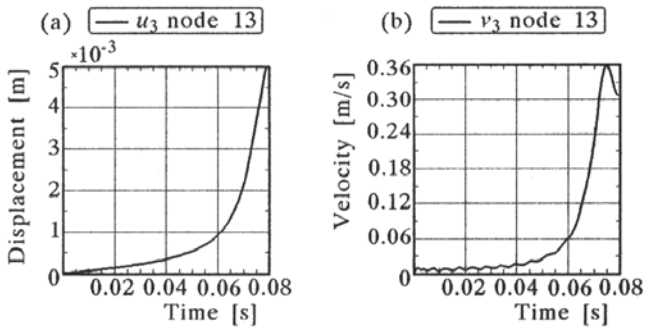

Fig. 9. Time history of deflection (a) and deflection velocity (b) for $h_2 = 0.02\,\mathrm{m}$ and $G_2 = 15.82\,\mathrm{MPa}$

Table 3 presents detailed results of the critical time t_{cr} and deflection w_{dcr}.

Table 3. Values of the critical time t_{cr} and critical deflection w_{dcr} for the analysed examples of plates

Parameters of the plate core h_2 [m]/G_2 [MPa]	t_{cr} [s]	w_{dcr} [m]
0.005/5.0	0.02	$4.38 \cdot 10^{-3}$
0.02/5.0	0.034	$3.56 \cdot 10^{-3}$
0.06/5.0	0.069	$4.8 \cdot 10^{-3}$
0.005/15.82	0.031	$4.31 \cdot 10^{-3}$
0.02/15.82	0.075	$3.88 \cdot 10^{-3}$

Examplary forms of axially symmetrical deformations of the plate with core thickness $h_2 = 0.005\,\mathrm{m}$ and $h_2 = 0.06\,\mathrm{m}$ are shown in Fig. 10.

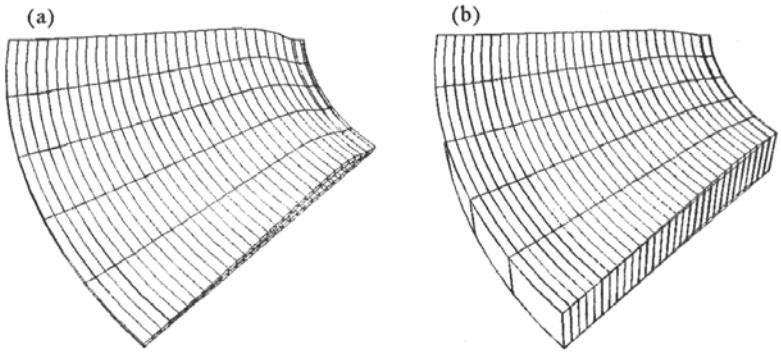

Fig. 10. Deformation of the plate with core thickness: (a) $h_2 = 0.005\,\mathrm{m}$, (b) $h_2 = 0.06\,\mathrm{m}$

The critical time and deflections for plates with the core mesh built of two solid element layers (Fig. 3b) do not differ essentially for most of the results. They are presented in Table 4. The major difference is only observed for the critical time and deflection of the plate with a thick core ($h_2 = 0.06\,\mathrm{m}$). These values are about 5% and 10% less than the critical time and deflection obtained for the plate with the single element layer of the core mesh.

Table 4. Values of the critical time t_{cr} and deflection w_{dcr} for plates with double element layers of the core mesh

Parameters of the plate core h_2 [m]/G_2 [MPa]	t_{cr} [s]	w_{dcr} [m]
0.005/5.0	0.02	$4.38 \cdot 10^{-3}$
0.02/5.0	0.034	$3.57 \cdot 10^{-3}$
0.06/5.0	0.067	$4.42 \cdot 10^{-3}$
0.005/15.82	0.031	$4.31 \cdot 10^{-3}$
0.02/15.82	0.075	$3.9 \cdot 10^{-3}$

Exemplary time histories of deflection and velocity of deflection of the plate with the core mesh built of the double element layers are shown in Fig. 11. The core thickness is $h_2 = 0.005\,\mathrm{m}$ and Kirchhoff's modulus of the core material is $G_2 = 5\,\mathrm{MPa}$.

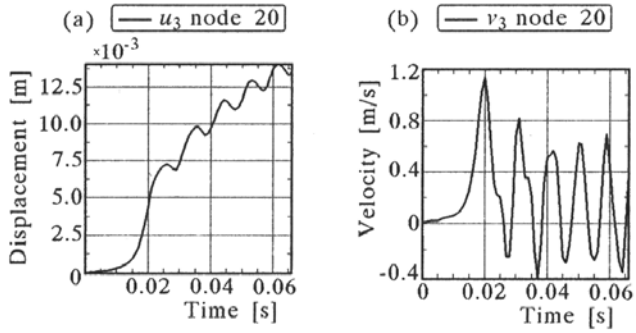

Fig. 11. Time history of deflection (a) and deflection velocity (b) for the plate with the double element layers of the core mesh

Calculations made with the help of the Finite Element Method enable evaluation of distribution of maximum stresses in plate layers. Examplary distribution of von Mises equivalent stresses in the plate facing and core shearing stresses in the xz plane (Fig. 1), calculated at the centroid of the element,

are presented in Fig. 12 and Fig. 13, respectively. The obtained results are for a plate with core thickness $h_2 = 0.005\,\mathrm{m}$ and core Kirchhoff's modulus $G_2 = 5.0\,\mathrm{MPa}$.

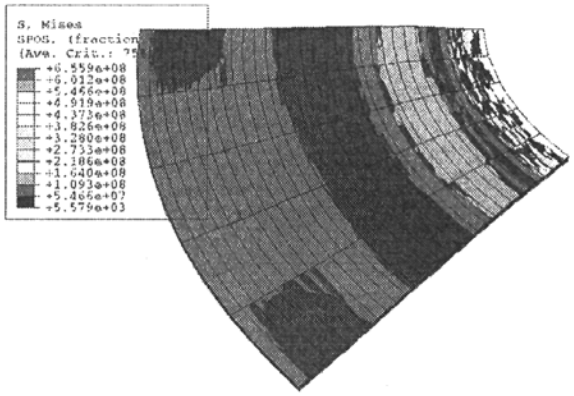

Fig. 12. Distribution of von Mises equivalent stresses in the facing

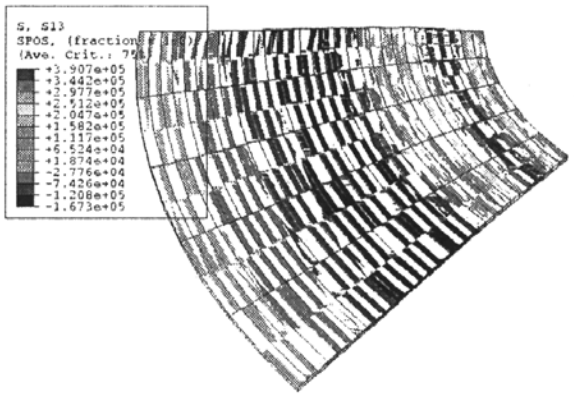

Fig. 13. Distribution of core shearing stresses in the xz plane

5. Results discussion

The obtained results concerning plates of different core thicknesses and core materials for both calculation methods indicate the increase in the critical time t_{cr} up to the loss of plate dynamic stability and obvious increase in the critical dynamic loading p_{crdyn} with the increase in both core thickness and Kirchhoff's modulus of the core material.

In the supercritical region of plate loading, an increase in the core stiffness entails decay of vibrations initiated by the increasing loading.

The values of critical maximum deflections w_{dcr} are in the range from 0.0033 m to 0.0052 m. The critical time t_{cr} calculated by both methods are comparable. The percentage relative differences in the critical time t_{cr} and connected with them values of the critical, dynamic loading are in a range 10% lower for plates with a thicker core ($h_2 = 0.06$ m) and higher for plates with a thinner core ($h_2 = 0.005$ m).

The modification of the finite element model of the plate from the single layer of core elements to double layers does not influence on calculation results, indeed. For plates with thinner ($h_2 = 0.005$ m) and medium ($h_2 = 0.02$ m) cores the values of critical times are identical and the maximum plate deflection differs insignificantly. Plates with a thick core ($h_2 = 0.06$ m) lose their dynamic stability slightly earlier; the value of the critical maximum deflection is lower. The compatibility of obtained results could confirm the correctness of the calculation model structure in Finite Element Method.

In stress state analysis, the calculation results could complete the analysis of plates solved a finite difference method. Using equation (2.1) and the critical time t_{cr}, the dynamic loads were calculated (presented in Table 2), which determine the radial membrane stresses of the inner plate edge. The values of membrane stresses are in the range from 100 MPa for thin and soft plate cores ($h_2 = 0.005$ m, $G_2 = 5$ MPa) to a rather significant value of 350 MPa for a plate with thicker and stiffer cores ($h_2 = 0.02$ m, $G_2 = 15.82$ MPa).

A complete stress state analysis with von Mises equivalent stresses in the plate facing and core shearing stresses in the xz plane (Fig. 1) determined at the moment of loss of dynamic stability is presented by results obtained by means of the finite element method. They are shown for an exemplary plate in Fig. 12 and Fig. 13. The values of critical von Mises stresses in the outer layer are in the range of 600 MPa in the area of the loading plate edge. In the buckling area of plate deformation, the stress is about 170 MPa. The critical maximum core shearing stress is rather significant, too. Its value is about 0.39 MPa.

6. Conclusions

Presented in this paper results of calculations carried out for a three-layered annular plate with a soft elastic core enable evaluation of the critical and supercritical behaviour of the plate subjected to a linear rapidly growing lateral

loading. In terms of qualitative and quantitative analysis, the results obtained as solutions to presented computational models of plates are comparable. Certain participation of normal stresses carried by the core and no connection with the condition of equal deflections between the plate layers in the model built in the finite elements method are the basic differences between the considered calculations. It seems, however, that the mentioned differences in model structures do not essentially influence on the final results. Therefore, the indicated calculation methods could complement each other in the analysis of the considered dynamic stability problem of a sandwich plate with an elastic core. The obtained examplary results enable one to know the plate behaviour and evaluate important values of critical parameters.

The presented analysis refers to examples of plates with elastic cores. At this stage of analysis, rheological properties of the polyurethane foam core material has not been taken into consideration. Therefore, the obtained results concern solutions to the cases of plates subjected to instantaneous loadings. The observed in preliminary analysis influence of rheological properties of the core material on time histories of plate deflections appears for a loading increasing in an adequately long time with considerably lower speed than it is assumed in the present work. The solution to the problem including rheological properties of the core material could be a subject of future analysis, initially indicated by Pawlus (2002b, 2003c).

References

1. ABAQUS/Standard. User's Manual, version 6.1, 2000, Hibbitt, Karlsson and Sorensen, Inc.

2. DUMIR P.C., SHINGAL L., 1985, Axisymmetric postbuckling of orthotropic thick annular plates, *Acta Mechanica*, **56**, 229-242

3. DUMIR P.C., JOSHI S., DUBE G.P., 2001, Geometrically nonlinear axisymmetric analysis of thick laminated annular plate using FSDT, *Composites: Part B*, **32**, 1-10

4. KLUESENER M.F., DRAKE M.L., 1982, Mathematical modeling. Damped structure design using finite element analysis, *Shock and Vibration Bulletin*, **52**, 1-12

5. MAJEWSKI S., MAĆKOWSKI R., 1975, Pełzanie spienionych tworzyw sztucznych stosowanych jako rdzeń płyt warstwowych, *Inżynieria i Budownictwo*, **3**, 127-131

6. PAWLUS D., 2000, Numerical solutions of deflections of linear viscoelastic, annular plates under lateral variable loads, *Machine Dynamics Problems*, **24**

7. PAWLUS D., 2002a, Obliczenia statycznych obciążeń krytycznych trójwarstwowych, osiowosymetrycznych płyt pierścieniowych, *Czasopismo Techniczne*, **6-M**, Wydawnictwo Politechniki Krakowskiej, 71-86

8. PAWLUS D., 2002b, Three-layered annular plate under lateral variable loads, *Proceedings of the International IASS Symposium on Lightweight Structures in Civil Engineering*, Warsaw, Poland, June, 2002

9. PAWLUS D., 2003a, Calculations of three-layered annular plates under lateral loads, *Studia Geotechnica et Mechanica*, **XXV**, 3-4

10. PAWLUS D., 2003b, Obliczenia metodą elementów skończonych krytycznych obciążeń statycznych trójwarstwowych płyt pierścieniowych, *Czasopismo Techniczne*, **6-M**, Wydawnictwo Politechniki Krakowskiej, 137-150

11. PAWLUS D., 2003c, Stateczność dynamiczna warstwowych płyt pierścieniowych z rdzeniem sprężystym i lepkosprężystym, *X Sympozjum Stateczności Konstrukcji*, Zakopane, Sept. 2003, 359-366

12. ROMANÓW F., 1995, *Wytrzymałość konstrukcji warstwowych*, WSI w Zielonej Górze

13. TANOV R., TABIEI A., 1998, Static and dynamic buckling of laminated composite shells, *Proceedings of the 5-th International LS-DYNA Users Conference*, South Field, MI, Sept. 1998

14. TANOV R., 2000, A contribution to the finite element formulation for the analysis of composite sandwich shells, Ph.D. Thesis, University of Cincinnati

15. TROMBSKI M., 1972, Zagadnienie płyt pierścieniowych o ortotropii cylindrycznej w ujęciu nieliniowym, *Zeszyty Naukowe Politechniki Łódzkiej*, **32**

16. TROMBSKI M., WOJCIECH S., 1981, Płyta pierścieniowa o ortotropii cylindrycznej obciążona w swej płaszczyźnie ciśnieniem zmiennym w czasie, *The Archive of Mechanical Engineering*, **XXVIII**, 2

17. TYLIKOWSKI A., 1989, Dynamic stability of viscoelastic shells under time dependent membrane loads, *International Journal of Mechanical Sciences*, **31**, 8

18. VOLMIR C., 1967, *Stability of Deformed System*, Science, Moskwa (in Russian)

19. VOLMIR C., 1972, *Nonlinear Dynamic of Plates and Shells*, Science, Moskwa (in Russian)

20. WOJCIECH S., 1978, Stateczność dynamiczna ortotropowej płyty pierścieniowej obciążonej w swojej płaszczyźnie ciśnieniem zmiennym w czasie, Ph.D. Thesis, Politechnika Łódzka

21. WOJCIECH S., 1979, Numeryczne rozwiązanie zagadnienia stateczności dynamicznej płyt pierścieniowych, *Journal of Theoretical and Applied Mechanics*, **17**, 2

Zagadnienie stateczności dynamicznej trójwarstowowych płyt pierścieniowych poddanych w płaszczynie obciążeniom zmiennym w czasie

Streszczenie

W pracy przedstawione zostały rozwiązania wykorzystujące metodę różnic skończonych oraz metodę elementów skończonych trójwarstwowych płyt pierścieniowych obciążonych szybko narastającym w czasie ciśnieniem działającym na wewnętrzny brzeg płyty. Rozwiązania płyt wraz z przykładowymi wynikami obliczeń przedstawiono dla przypadku osiowosymetrycznej postaci utraty stateczności płyty dwustronnie utwierdzonej przesuwnie o symetrycznym układzie warstw poprzecznych: zewnętrznych cienkich okładzinach i piankowym, miękkim, grubszym rdzeniu. Wykorzystując metodę różnic skończonych wyprowadzono podstawowy układ równań różniczkowych analizowanej płyty umożliwiający wyznaczanie jej postępujących ugięć w czasie obciążania. W metodzie elementów skończonych zbudowano model obliczeniowy pierścieniowego wycinka płyty zapewniający warunki pracy płyty trójwarstwowej z rdzeniem miękkim. Wyniki obliczeń dynamicznych przedstawiono w postaci charakterystyk maksymalnych ugięć i ich prędkości. Wyniki obliczeń przykładowych płyt różniących się grubością i sztywnością piankowego rdzenia umożliwiają obserwację krytycznych i pokrytycznych zachowań płyt wraz z ilościową oceną wartości parametrów krytycznych: czasu, ugięcia i obciążenia dynamicznego wyznaczonych wykorzystując kryterium podane w pracy Volmira (1972).

Manuscript received November 28, 2004; accepted for print December 6, 2004